Tubular Injury in a Rat Model of Type 2 Diabetes Is Prevented by Metformin

A Possible Role of HIF-1α Expression and Oxygen Metabolism

Yumi Takiyama,[1] Tatsuo Harumi,[2] Jun Watanabe,[1] Yukihiro Fujita,[1] Jun Honjo,[1] Norihiko Shimizu,[3] Yuichi Makino,[1] and Masakazu Haneda[1]

OBJECTIVE—Chronic hypoxia has been recognized as a key regulator in renal tubulointerstitial fibrosis, as seen in diabetic nephropathy, which is associated with the activation of hypoxia-inducible factor (HIF)-1α. We assess here the effects of the biguanide, metformin, on the expression of HIF-1α in diabetic nephropathy using renal proximal tubular cells and type 2 diabetic rats.

RESEARCH DESIGN AND METHODS—We explored the effects of metformin on the expression of HIF-1α using human renal proximal tubular epithelial cells (HRPTECs). Male Zucker diabetic fatty (ZDF; Gmi-*fa/fa*) rats were treated from 9 to 39 weeks with metformin (250 mg · kg^{-1} · day^{-1}) or insulin.

RESULTS—Metformin inhibited hypoxia-induced HIF-1α accumulation and the expression of HIF-1–targeted genes in HRPTECs. Although metformin activated the downstream pathways of AMP-activated protein kinase (AMPK), neither the AMPK activator, AICAR, nor the mTOR inhibitor, rapamycin, suppressed hypoxia-induced HIF-1α expression. In addition, knockdown of AMPK-α did not abolish the inhibitory effects of metformin on HIF-1α expression. The proteasome inhibitor, MG-132, completely eradicated the suppression of hypoxia-induced HIF-1α accumulation by metformin. The inhibitors of mitochondrial respiration similarly suppressed hypoxia-induced HIF-1α expression. Metformin significantly decreased ATP production and oxygen consumption rates, which subsequently led to increased cellular oxygen tension. Finally, metformin, but not insulin, attenuated tubular HIF-1α expression and pimonidazole staining and ameliorated tubular injury in ZDF rats.

CONCLUSIONS—Our data suggest that hypoxia-induced HIF-1α accumulation in diabetic nephropathy could be suppressed by the antidiabetes drug, metformin, through the repression of oxygen consumption. ***Diabetes*** **60:981–992, 2011**

Diabetic nephropathy now is a leading cause of end-stage renal failure and therefore constitutes a major component of progressive kidney disease. Chronic hypoxia and tubulointerstitial fibrosis presently are considered to be common pathways for various progressive kidney diseases, including diabetic nephropathy, and hypoxia-inducible factor (HIF)-1α plays an important role in these pathological mechanisms (1–4). Recent studies (4–6) have demonstrated that hypoxia represents an early event in the development and progression of diabetic nephropathy and an increase in HIF-1α expression in diabetic kidneys compared with the kidneys of control rats (7) and normal human kidneys (8). In addition, Higgins et al. (8) have demonstrated that HIF-1α enhanced the epithelial-to-mesenchymal transition (EMT) in vitro and that genetic ablation of renal epithelial HIF-1α inhibited the development of tubulointerstitial fibrosis using HIF-1α knockout mice. Sun et al. (9) further provided a novel explanation for the EMT of hypoxic renal tubular cells through the upregulation of Twist induced by HIF-1α. Kimura et al. (10) recently showed that stable expression of HIF-1α in tubular epithelial cells promotes interstitial fibrosis in knockout mice with von Hippel-Lindau (VHL) tumor suppressor, which acts as an ubiquitin ligase to promote proteolysis of HIF-α.

Metformin has been widely used for treating type 2 diabetes without the stimulation of insulin production, and, for this reason, it is considered an insulin sensitizer (11). The UK Prospective Diabetes Study (UKPDS) showed that metformin could reduce macrovascular morbidity and mortality (12), suggesting that it achieved its antiatherogenic and anti-inflammatory effects by means of antioxidant properties (13). Moreover, metformin significantly decreased the urine albumin excretion rate in patients with type 2 diabetes (14). The benefits of metformin with regard to the risk of cardiovascular outcomes and metabolic parameters suggest its clinical use in treating chronic kidney disease (15). The precise mechanisms beyond the effects of metformin on glucose still are obscure. Recently, metformin has been found to activate AMP-activated protein kinase (AMPK), a major cellular regulator of lipid and glucose metabolism (16,17), via a liver kinase B1 (LKB1)-dependent mechanism (18). The LKB1-AMPK–mammalian target of rapamycin (mTOR) pathway is a key regulator of HIF-1–targeted genes and HIF-1–mediated cellular metabolism (19–21). In addition, a recent study (22) has shown that metformin inhibits insulin and IGF-1–induced HIF-1α expression in nontumor retinal epithelial ARPE-19 cells. This evidence led us to question whether metformin, known as an AMPK activator, might regulate the expression of HIF-1α protein in renal proximal tubular cells. Therefore, we investigated the effects of metformin on HIF-1α expression using cultured human renal proximal

From the [1]Division of Metabolism and Biosystemic Science, Department of Medicine, Asahikawa Medical University, Asahikawa, Japan; the [2]Department of Anatomy, Asahikawa Medical University, Asahikawa, Japan; and the [3]Animal Laboratory for Medical Research, Asahikawa Medical University, Asahikawa, Japan.
Corresponding author: Yumi Takiyama, taka0716@asahikawa-med.ac.jp.
Received 8 May 2010 and accepted 28 December 2010.
DOI: 10.2337/db10-0655

tubular epithelial cells (HRPTECs) and Zucker diabetic fatty (ZDF) rats, a model of type 2 diabetes (23).

RESEARCH DESIGN AND METHODS

Metformin was provided by Dainippon Sumitomo Pharma (Osaka, Japan). AICAR, MG-132, and rapamycin were purchased from Calbiochem (San Diego, CA). Anti–AMPK-α, anti–AMPK-α1, anti–AMPK-α2, anti–phosphorylated (p)-AMPK-α (Thr172), anti–*p*-acetyl-CoA carboxylase (ACC) (Ser79), and anti–*p*-mTOR (Ser2448) antibodies were obtained from Cell Signaling Technology (Beverly, MA). The primary antibodies are monoclonal mouse antibodies for human HIF-1α (BD Biosciences, Benford, MA) and for rat HIF-1 α (Novus Biological, Littleton, CO). D-glucose was purchased from Wako Pure Chemical Industries (Osaka, Japan). ON-TARGETplus SMARTpool siControl (D-001810), AMPK-α1 (NM-006251), AMPK-α2 (NM-006252), and small-interference RNAs (siRNAs) were purchased from Dharmacon (Lafayette, CO). Alexa Fluor 594 donkey anti-mouse secondary antibody was purchased from Invitrogen (Gaithersburg, MD). Other chemicals and antibodies were obtained from Sigma-Aldrich (St. Louis, MO), unless otherwise indicated.

Human renal proximal epithelial tubular cell cultures. Human proximal tubular epithelial cells (HPRTECs) were purchased as once- or twice-passaged tubular cells from Lonza Walkersville (Walkersville, MD). The tubular cells were cultured in renal epithelial cell growth medium, according to the manufacturer's instructions, as described before (24). After 24 h of starvation with serum-free DMEM, the cells were exposed to reagents under normoxic (21% O_2) or hypoxic (1% O_2) conditions for ~4–24 h and were then harvested for experiments. In all, experiments were deprived of serum.

RNA isolation, RT-PCR, and real-time RT-PCR. Total RNA extraction and cDNA synthesis were preformed as described previously (24). Each cDNA sample was analyzed for gene expression by quantitative real-time PCR with an ABI 7300 Sequence Detector (Applied Biosystems, Foster City, CA) using the TaqMan Universal PCR Master Mix (Applied Biosystems), as described previously (24). Unlabeled specific primers were purchased from Applied Biosystems for detecting the human plasminogen activator inhibitor *(PAI)-1 (Serpine)* gene (assay ID no. HS00167155-ml), the human *SLC2A1* gene (assay ID no. HS00197884-ml), the human *HIF-1α* gene (assay ID no. HS00153153-ml), the human vascular endothelial growth factor (*VEGF*) gene (assay ID no. HS00900054-ml), and the *18S* gene (assay ID no. HS 9999991-sl).

siRNA and HRPTEC transfection. Silencing of *AMPK-α1/-α2* gene expression in HRPTECs was achieved by the siRNA technique, as described previously (24). Forty-eight hours after transfection, HRPTECs were serum starved for an additional 24 h and subsequently treated as indicated.

Protein extraction and Western blot analysis of intracellular proteins in HRPTECs. Total cellular extracts from HRPTECs were prepared, and Western blot was carried out using a denaturing 8% Novex Tris-glycine gels (Invitrogen, Carlsbad, CA) or 10% NuPage Bis-Tris SDS-PAGE gels under reducing conditions, as described previously (24). Membranes were washed and reprobed with an antibody against α-actinin (Sigma) to control for small variations in protein loading and transfer. Images were acquired using the Adobe Photoshop program (Adobe Systems, San Jose, CA) and processed using Multi Guage (Fuji Film, Tokyo, Japan) for densitometric analysis. Signal intensities in control lanes were arbitrarily assigned a value of 1.00.

Oxygen consumption measurements. Cells were incubated under normoxic (21% O_2) or hypoxic (1% O_2) conditions in medium containing 5.5 mmol/L (low) or 25 mmol/L (high) glucose and then resuspended in normoxic medium. Average oxygen consumption rates in HRPTECs treated with reagents in normoxia or hypoxia for 4 h were measured in a sealed chamber using a Clark-type electrode.

Measurement of cell ATP. HRPTECs were incubated with reagents under normoxic or hypoxic conditions for 4 h. ATP production was monitored by glucose-6-phosphate formation. Briefly, cells were extracted with perchloric acid (6%) and centrifuged (8,000*g* for 10 min). Subsequently, the extract was neutralized with K_2CO_3 (5 mol/L) neutralized to pH 7. $NADP^+$ (0.5 mmol/L) and glucose 6-phosphate dehydrogenase (0.25 units) were then added and ATP production was monitored from the NADPH content by spectrophotometry at 340 nm. Cell proteins were determined in parallel dishes for the normalization of the ATP values.

Imaging of reactive oxygen species. The oxidative fluorescent dihydroethidium (DHE) (Sigma) was used to evaluate the intracellular production of superoxide (O_2^-) (25). In brief, after incubation overnight, cells with or without 1 mmol/L metformin or 1 mmol/L AICAR under normoxic and hypoxic conditions were washed with serum-free and phenol-red–free DMEM and loaded with 5 μmol/L DHE. After incubation for 10 min in the dark, the cells were washed with PBS and were subjected to fluorescence microscopy.

NADPH content. NADPH content was determined using a NADP/NADPH Quantification kit (BioVision, Mountain View, CA) and the protocol supplied by the manufacturer.

Immunocytochemistry. HRPTECs were cultured on four-chamber glass slides (BD Biosciences) to reach 80% confluence. After exposure to 1 mmol/L metformin or 1 mmol/L AICAR for 4 h under normoxic or hypoxic conditions, the cells were fixed with 100% ethanol for 10 min and were incubated with an anti–HIF-1α antibody (1:100; BD Biosciences) at 4°C overnight. Then, cells were rinsed in PBS and subsequently incubated with Alexa Fluor 594 donkey anti-mouse secondary antibody (Invitrogen) at 1:200 dilution overnight at 4°C. Finally, slides were analyzed by cofocal laser–scanning microscopy.

Detection of cellular hypoxia. Cellular hypoxia was detected by adding pimonidazole hydrochloride (200 mmol/L hypoxyprobe-1; Hydroxyprobe, Burlington, MA), which binds to cells or tissues with pO_2 levels <10 mmHg, to HRPTECs that were treated with 1 mmol/L metformin or 1 mmol/L AICAR and exposed to hypoxia (1% O_2) for 4 h. To detect hypoxic conditions in each group of rats, pimonidazole (60 mg/kg) was injected intraperitoneally 1 h before they were killed. Staining was performed according to the manufacturer's instructions.

Animals. Male ZDF/Gmi-*fa/fa* rats and their heterozygous (ZDF/Gmi-+/*fa*) lean littermates were purchased from Charles River Japan. Animals purchased at 7 weeks of age were given an ad libitum commercial pellet diet (CE-2; CLEA, Tokyo, Japan) and tap water. ZDF rats were randomly assigned to four groups at the age of 9 weeks. A first group did not receive an active pharmacological treatment and was used as a control (ZDF control). A second group received metformin in standard diet at a concentration of 3.3 g/kg (ZDF+M group). Taking into account an average daily food intake of 32.4 g per rat, a dose of ~253.2 mg · kg^{-1} · day^{-1} was achieved. The metformin dose is compatible with those used in previous studies in rats (26,27). A third group was treated with a sustained-release insulin implant (~2 units per day per implant) (ZDF+I group) (Lin Shin Canada, Ontario, Canada). Heterozygous animals without active treatment were used as nondiabetic, lean controls (ZL group). Tail postprandial glucose in whole blood was quantified using a glucose analyzer (One Touch; Life Scan, Johnson & Johnson, Milpitas, CA). Hemoglobin A_{1c} was measured using the DCA 2000 analyzer (Siemens Medical Solutions Diagnostics, Tokyo, Japan). Renal function was assessed by measuring urinary albumin excretion. Urinary albumin was quantified using the Nephrat kit (Exocell, Philadelphia, PA), according to manufacturer's instructions. Animals were killed at the age of 17 weeks for pimonidazole staining and at the age of 39 weeks for assessment of morphology and immunohistochemistry for HIF-1α by overanesthetization with isoflurane and cardiac puncture. The kidneys were fixed with perfusion, as described in a previous study (28). The Asahikawa Medical College Research Center for Animal Life Science approved all experiments.

Morphological analysis and immunohistochemistry. To evaluate HIF-1α or pimonidazole expression in the kidney, immunohistochemistry was performed with mouse monoclonal anti–HIF-1α antibody (ESEE 122, 1:100) or mouse antipimonidazole (1:1000), as described previously (24). The positive immunoreactivity for nuclear HIF-1α protein or cytosolic pimonidazole was estimated as absent (0) for 0%, low (1) for 1–20%, intermediate (2) for 21–50%, and high (3) for more than 50% of the tubular cells in the juxtamedullary cortical and outer medullar regions. Assessment of tubulointerstitial injury was evaluated in the juxtamedullary cortical and outer medullar regions using periodic acid–Schiff staining and a semiquantitative scoring system evaluating interstitial fibrosis, inflammation, tubular atrophy, tubular dilation, debris accumulation, and cast formation. A score of 0 means normal tubulointerstitium, 1 means injury in <25%, 2 means injury in up to 50%, and 3 means injury in >50% of the biopsy specimen.

Statistical analysis. Three separate experiments at least were performed per protocol. Each treatment group was assayed in duplicate for real-time RT-PCR. The values shown represent the means ± SD. Statistical analysis was performed by ANOVA and Bonferroni post hoc tests. Values of $P < 0.05$ were considered statistically significant.

RESULTS

Metformin inhibits hypoxia-induced HIF-1α protein accumulation. We investigated the impact of metformin on hypoxia-induced HIF-1α expression. HRPTECs faintly expressed HIF-1α protein under normoxic condition (Fig. 1*A*). The treatment of hypoxia (1% O_2) markedly induced HIF-1α protein accumulation in HRPTECs, and metformin, at the concentration of 1 mmol/L, inhibited hypoxia-induced HIF-1α protein expression (Fig. 1*A*). Densitometric analysis showed that hypoxia significantly induced HIF-1α protein expression compared with the control in normoxia ($P < 0.01$) and a significant ~85% attenuation in hypoxia-induced HIF-1α protein accumulation in HRPTECs treated with 1 mmol/L metformin, compared with hypoxia-treated

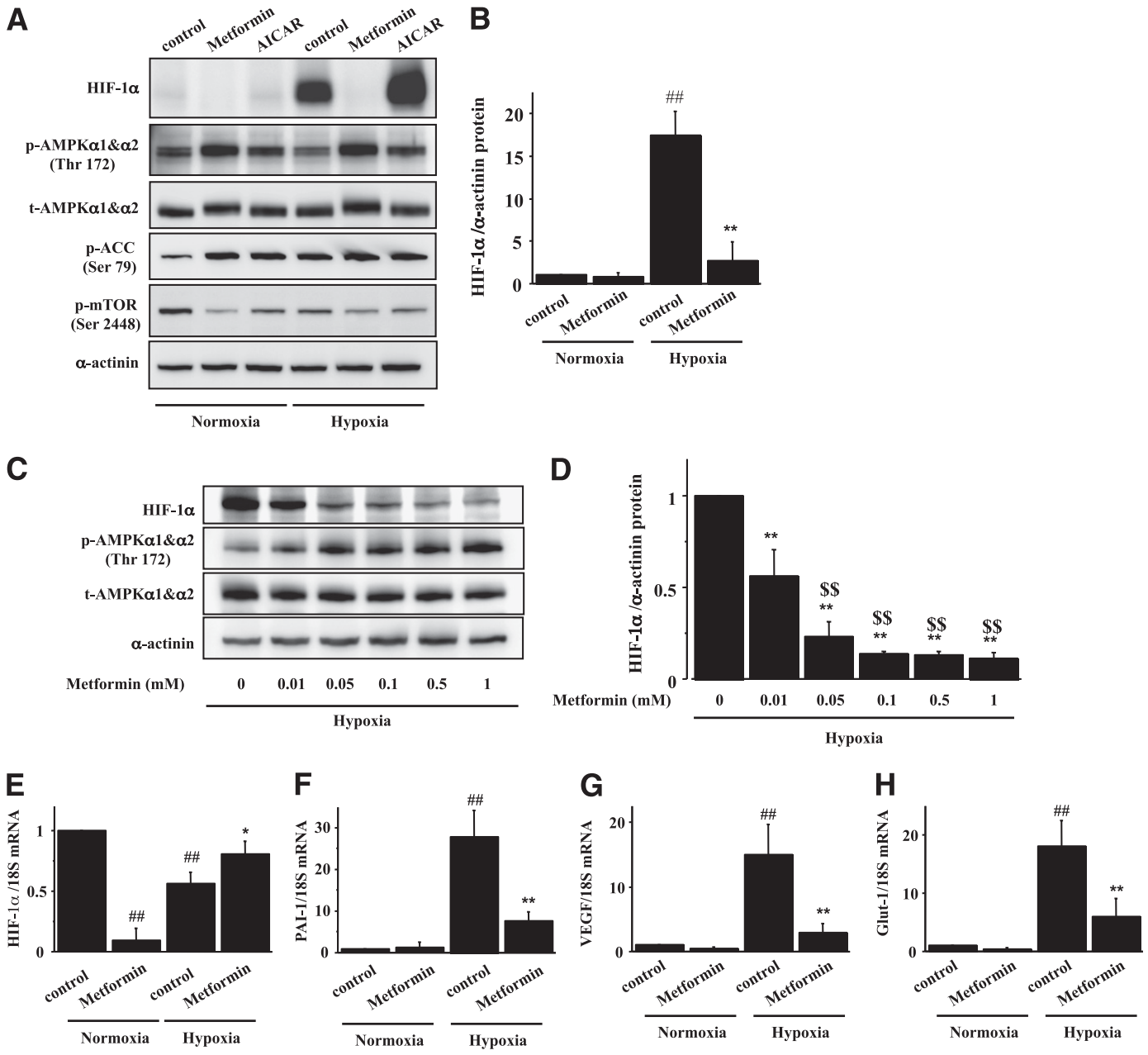

FIG. 1. ***A*: Metformin inhibits hypoxia-induced HIF-1α protein expression. HRPTECs were treated with 1 mmol/L metformin and 1 mmol/L AICAR under normoxic and hypoxic conditions overnight. Whole-cell protein extracted from HRPTECs was analyzed by Western blot analysis. Although AICAR stimulated the phosphorylation of AMPK and ACC and inhibited the phosphorylation of mTOR much like metformin, AICAR failed to suppress hypoxia-induced HIF-1α expression. *B*: Metformin inhibits hypoxia-induced HIF-1α protein expression. HRPTECs were treated with or without 1 mmol/L metformin under normoxic (21% O_2) and hypoxic (1% O_2) conditions overnight. Whole-cell proteins were extracted and analyzed for HIF-1α expression by Western blot. Metformin inhibited hypoxia-induced HIF-1α expression. Densitometric analysis showed that hypoxia significantly induced HIF-1α protein expression compared with that in control in normoxia and that metformin decreased hypoxia-induced HIF-1α expression to ~15.4% of that of control in hypoxia. ##$P < 0.01$ vs. control under normoxic conditions; **$P < 0.01$ vs. control under hypoxic conditions. *C*: Metformin inhibits hypoxia-induced HIF-1α accumulation. HRPTECs were incubated in serum-free DMEM with 0.01–1 mmol/L metformin under hypoxic conditions. After 4 h, cells were harvested for Western blot analysis. *D*: The inhibitory effect of metformin on hypoxia-induced HIF-1α expression was significantly detectable at 0.01 mmol/L. **$P < 0.01$ vs. control under hypoxic conditions; $$$P < 0.01$ vs. 0.01 mmol/L metformin-treated cells under hypoxic conditions. *E–H*: Quantitative real-time RT-PCR analysis of *HIF-1α* and *HIF-1* target genes. HRPTECs were treated with or without 10 mmol/L metformin under normoxic and hypoxic conditions overnight. Then, total RNA was extracted from HRPTECs and was applied for quantitative RT-PCR. The relative amounts of PAI-1, VEGF, and Glut-1 mRNA were normalized by 18S and expressed as an arbitrary unit in which the control group value equaled 1. Hypoxia significantly induced PAI-1, VEGF, and Glut-1 mRNA expression in HRPTECs, and 10 mmol/L metformin inhibited the induction of this mRNA expression by hypoxia. Data represent means ± SD ($n = 3$). ##$P < 0.01$ vs. control under normoxic conditions; *$P < 0.05$; **$P < 0.01$ vs. control under hypoxic conditions.**

controls ($P < 0.01$) (Fig. 1*B*). The inhibitory effect of metformin was detected at the concentration of 10 μmol/L, which was a therapeutic concentration as described in previous studies (11,29) (Fig. 1*C* and *D*), and for the incubation time of ~4–24 h (data not shown). In contrast, HIF-1α mRNA levels were not reduced by metformin in hypoxia, suggesting that metformin decreased HIF-1α protein via posttranslational mechanisms (Fig. 1*E*).

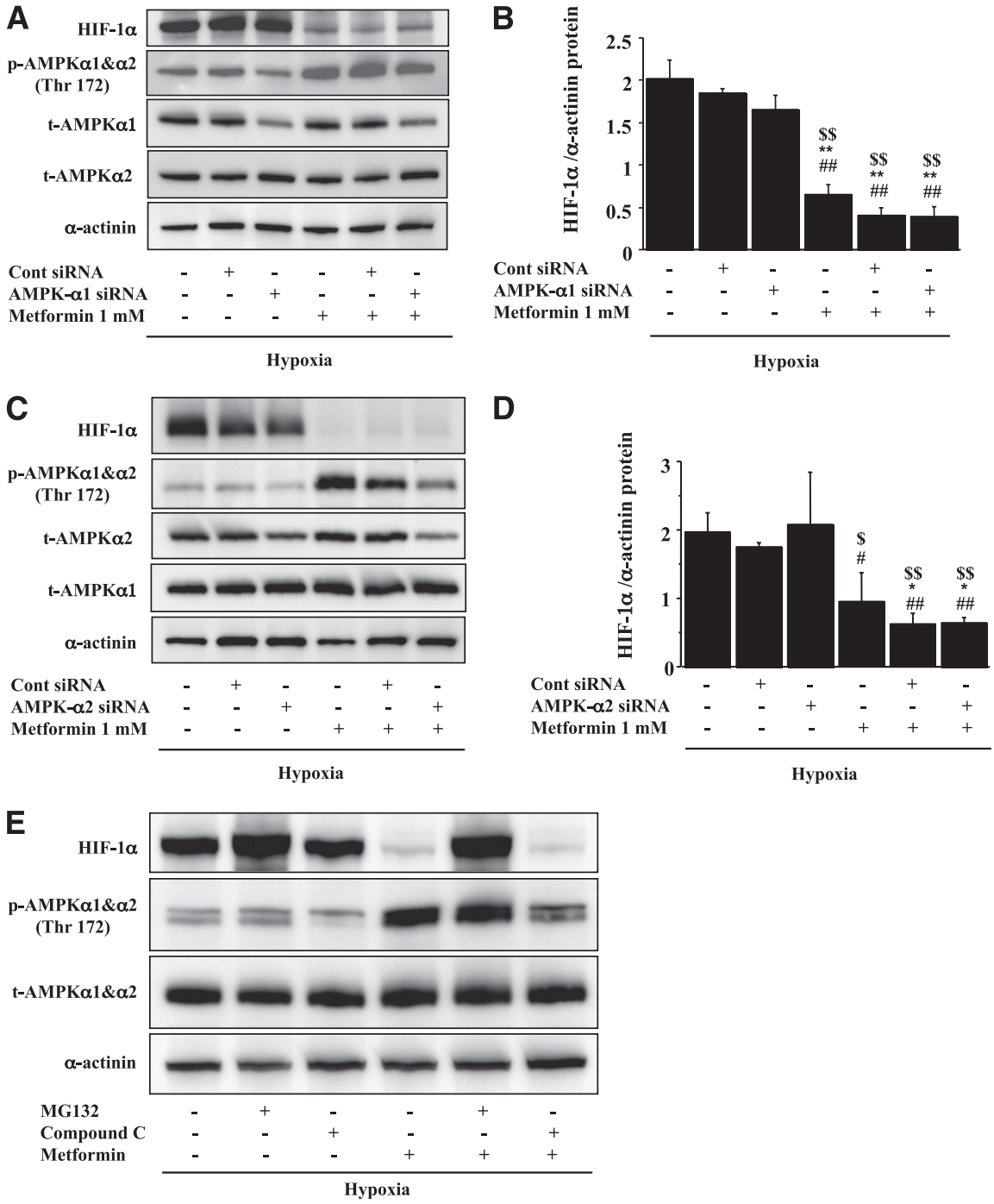

FIG. 2. Metformin inhibited hypoxia-induced HIF-1α protein expression independent of AMPK. *A–D*: HRPTECs were transiently transfected with control, AMPK-α1–, or -α2–specific siRNAs (25 nmol/L final concentration). Forty-eight hours after transfection, cells were serum starved for an additional 24 h and subsequently treated as indicated under normoxic or hypoxic conditions for 4 h, and cells were lysed and subjected to immunoblotting with specific antibodies indicated. Lowering AMPK-α1 (*A* and *B*) or AMPK-α2 (*C* and *D*) protein expression with specific siRNA failed to restore the inhibitory effects of metformin on hypoxia-induced HIF-1α protein expression. #$P < 0.05$; ##$P < 0.01$ vs. nontreated cells; *$P < 0.05$; **$P < 0.01$ vs. control siRNA-transfected cells; \$$P < 0.05$; \$\$$P < 0.01$ vs. AMPK-α1 or -α2 siRNA-transfected cells under hypoxic conditions. *E*: The proteasomal inhibitor MG-132 (10 μmol/L) abolished the inhibitory effect of 10 mmol/L metformin on HIF-1α accumulation under hypoxic conditions for 4 h. Although an AMPK inhibitor, compound C (20 μmol/L) failed to antagonize the inhibitory effect of metformin on HIF-1α protein expression.

Metformin inhibits hypoxia-induced PAI-1, VEGF, and Glut-1 mRNA expressions. We examined the effects of metformin on the expression of HIF-1 target genes in HRPTECs (Fig. 1*F–H*). Real-time PCR results showed that hypoxia significantly promoted *PAI-1*, *VEGF*, and *Glut-1* gene expression in HRPTECs. Treatment with 10 mmol/L metformin significantly reduced the enhancing effects of hypoxia on these mRNA expressions.

Metformin inhibits hypoxia-induced HIF-1α expression independent of AMPK. As shown in Fig. 1*A* and *C*, metformin inhibited hypoxia-induced HIF-1α protein accumulation in HRPTECs, accompanied by increased AMPK-α

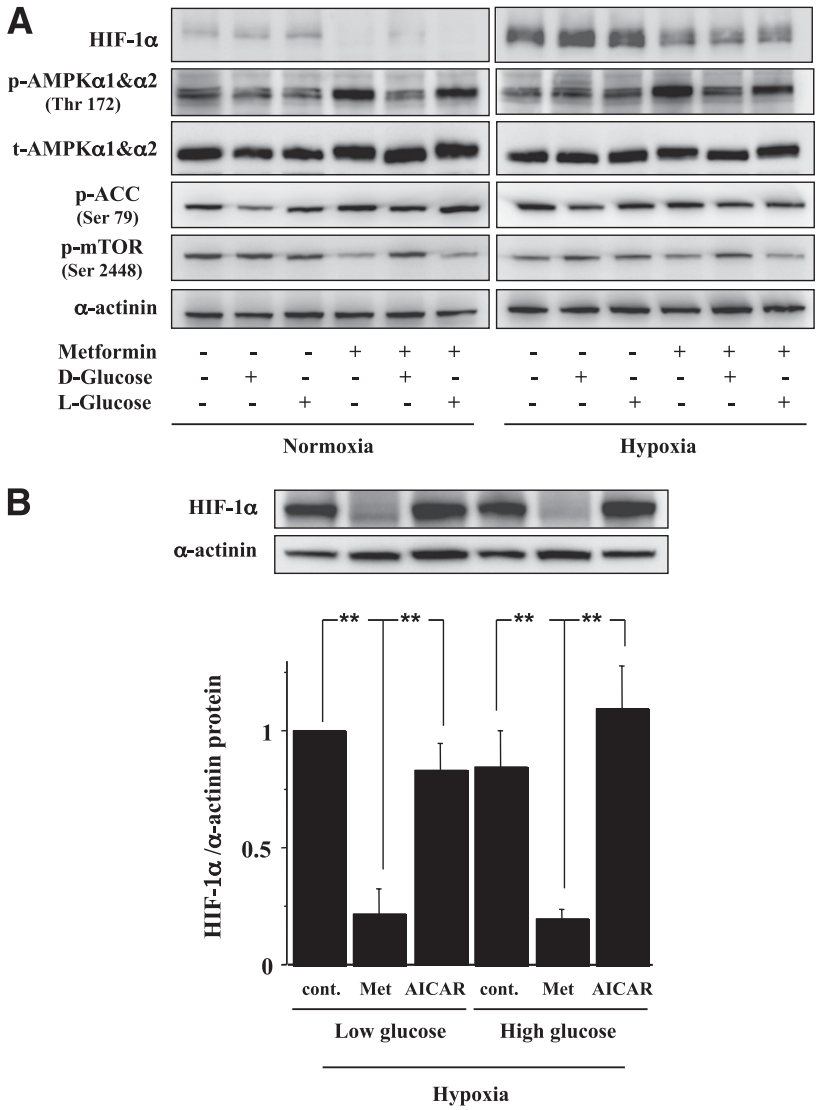

FIG. 3. Effects of high glucose on the inhibitory effects of metformin on hypoxia-induced HIF-1α expression. *A*: HRPTECs were treated with high D-glucose (25 mmol/L) and 1 mmol/L metformin under normoxic and hypoxic conditions overnight. Whole-cell proteins extracted from HRPTECs were then analyzed by Western blot. Although high glucose attenuated the stimulatory effects of metformin on the expression of *p*-AMPK and *p*-ACC and the inhibitory effects of metformin on the expression of *p*-mTOR, high glucose did not blunt the inhibitory effect of metformin on HIF-1α expression. L-glucose (25 mmol/L) as an osmolarity control also did not alter the effects of metformin. *B*: Densitometric analysis showed that high glucose did not affect HIF-1α protein expression in hypoxia and that metformin still decreased hypoxia-induced HIF-1α expression to >80% of that of control in hypoxia independent of glucose concentrations. **$P < 0.01$.

phosphorylation. We also determined the effects of an AMPK activator, AICAR, on hypoxia-induced HIF-1α expression (Fig. 1*A*). Although AICAR stimulated the phosphorylation of AMPK and ACC and inhibited the phosphorylation of mTOR-like metformin under normoxic and hypoxic conditions, AICAR failed to suppress hypoxia-induced HIF-1α expression (Fig. 1*A*). To study the role of AMPK on the inhibitory effects of metformin on HIF-1α expression, we have taken a genetic approach to inhibit the AMPK activity under hypoxic conditions. Immunoblots using antiphosphorylated (Thr172)-AMPK-α1 and -α2 antibody increased significantly in response to metformin dose dependently in siAMPK-α1–treated cells, suggesting that the presence of AMPK-α2 compensated for the absence of AMPK-α1 (Fig. 2*A*). In contrast, total *p*–AMPK-α content was markedly suppressed in siAMPK-α2–transfected cells treated with metformin (Fig. 2*C*), indicating that metformin could predominantly augment the phosphorylation of AMPK-α2 in HRPTECs, which was consistent with the previous study (30) investigating the effects of AICAR, hypoxia, and rotenone on isoform-specific AMPK activity. Thus, lowering the AMPK-α protein using specific siRNA for AMPK-α1 or -α2 did not affect hypoxia-induced HIF-1α expression and failed to abolish the inhibitory effects of metformin on hypoxia-induced HIF-1α expression (Fig. 2*A–D*).

Proteasomal inhibitor MG-132 pretreatment restores the inhibitory effects of metformin on hypoxia-induced HIF-1α expression. To examine the posttranslational regulation of HIF-1α protein by metformin, we used the proteasomal inhibitor MG-132. As shown in Fig. 2*E*, MG-132 restored the inhibitory effect of metformin on hypoxia-induced HIF-1α accumulation, indicating that metformin exhibited its inhibitory effect on HIF-1α accumulation by promoting proteasomal HIF-1α degradation. Although an AMPK inhibitor, compound C (20 μmol/L) failed to

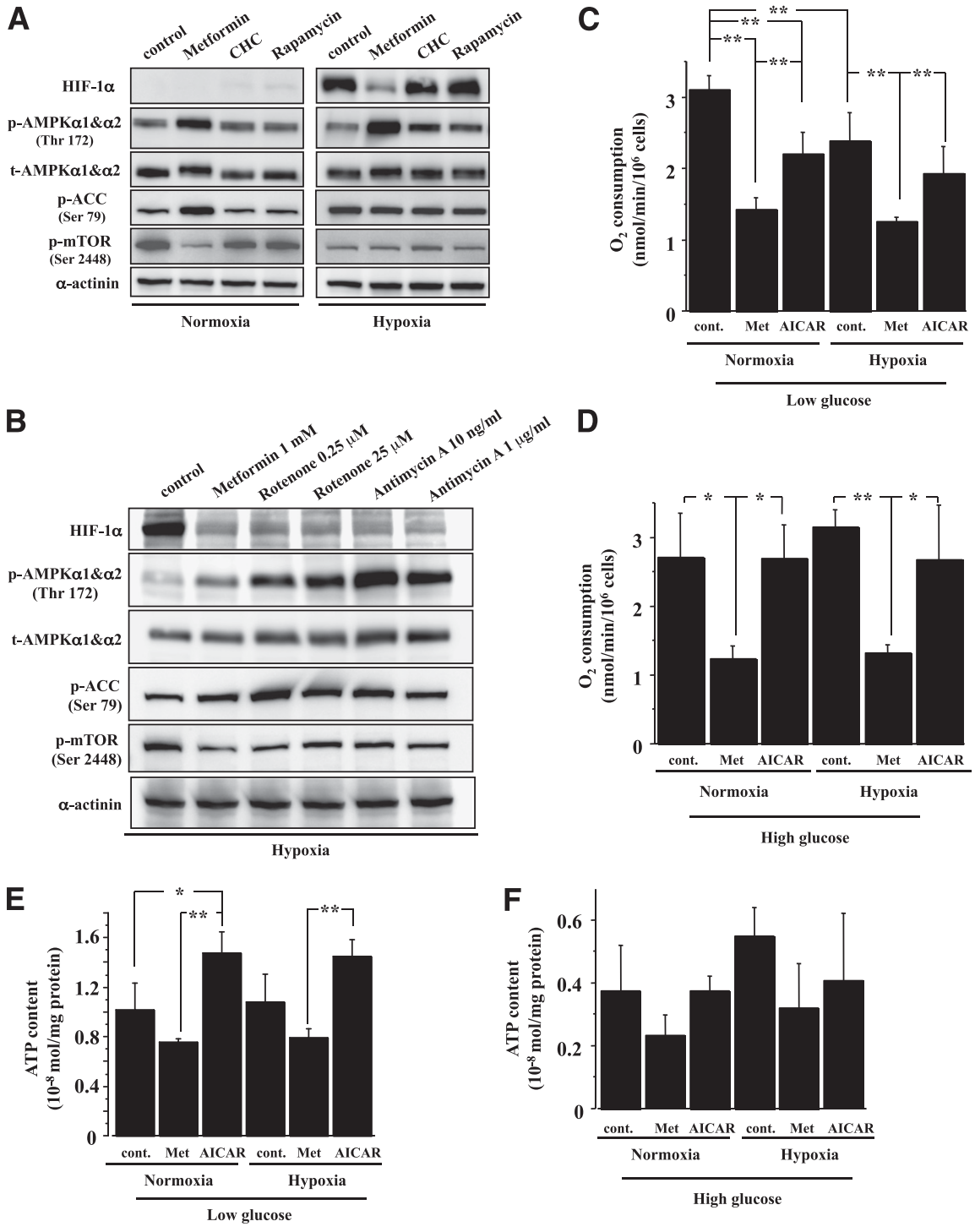

FIG. 4. ***A*****: Effects of inhibitors of mitochondrial pyruvate transport, mTOR, and mitochondrial respiratory complexes I and III on the expression of hypoxia-induced HIF-1α. HRPTECs were treated with inhibitors of mitochondrial pyruvate transport (0.1 mmol/L CHC), mTOR (100 nmol/L rapamycin), and with 1 mmol/L metformin under normoxic and hypoxic conditions for 4 h. These inhibitors failed to decrease hypoxia-induced HIF-1α accumulation.** ***B*****: The inhibitors for mitochondrial respiratory complexes I and III inhibit hypoxia-induced HIF-1α accumulation. The cells were treated with mitochondrial respiratory complex I (0.25 μmol/L, 25 μmol/L rotenone), mitochondrial respiratory complex III (10 ng/mL, 1 μg/mL antimycin A), and with 1 mmol/L metformin under hypoxic conditions for 4 h. The inhibition of mitochondrial respiration suppressed HIF-1α protein expression, accompanied with increased expressions of *p*-AMPK and *p*-ACC, and decreased *p*-mTOR expression.** ***C*** **and** ***D*****: Metformin suppressed mitochondrial respiratory functions of HRPTECs in normoxia and hypoxia in medium containing 5.5 mmol/L (low) (*C*) or 25 mmol/L (high) (*D*) glucose. Cells treated with indicated reagents were incubated in normoxia (21% O_2) or hypoxia (1% O_2) for 4 h and then resuspended in normoxic medium. Oxygen consumption was measured in a sealed chamber using a Clark-type electrode.** ***C*****: Hypoxia decreased oxygen consumption down to 76.5% of the control in normoxia in low glucose (**$P < 0.01$) (*C*).** ***D*****: This response to hypoxia was blunted by 25 mmol/L glucose. Metformin significantly inhibited oxygen consumption to <50% of controls, independent of the oxygen conditions or the glucose milieu (*$P < 0.05$; **$P < 0.01$). Data are expressed as means ± SD ($n = 3$).** ***E*** **and** ***F*****: Cell ATP during metformin or AICAR treatment under normoxia and hypoxia in medium containing 5.5 mmol/L (low) (*E*) or 25 mmol/L (high) (*F*) glucose. HRPTECs were incubated with indicated reagents in normoxia or hypoxia for 4 h. At the end of incubation, cells were extracted with perchloric acid for the measurement of ATP as described in RESEARCH DESIGN AND METHODS. Protein was determined in parallel dishes. Cell ATP was normalized with protein. Data are expressed as means ± SD ($n = 3$).** ***E*****: The**

antagonize the inhibitory effect of metformin on HIF-1α protein expression (Fig. 2*E*).

High glucose does not affect the inhibitory effects of metformin on hypoxia-induced HIF-1α expression. As shown in Fig. 3*A*, high glucose attenuated the stimulatory effects of metformin on the phosphorylation of AMPK-α and ACC and restored the inhibitory effect of metformin on *p*-mTOR expression. These results were similar to those of a recent study (31) in diabetic rats. However, the treatment of high glucose did not blunt the inhibitory effect of metformin on HIF-1α expression (Fig. 3*A* and *B*), concomitantly suggesting that the activation of AMPK-α is insufficient for the inhibitory effect of metformin on hypoxia-induced HIF-1α expression.

Mitochondrial respiratory complex inhibitors, but not rapamycin, mimic the actions of metformin on AMPK activation and hypoxia-induced HIF-1α expression. To determine the mechanism implicated in the regulation of HIF-1α expression in HRPTECs, subsequent experiments were achieved by the use of inhibitors of mitochondrial pyruvate transport (0.1 mmol/L α-cyano-4-hydroxycinnamate [CHC]), mTOR (100 nmol/L rapamycin), mitochondrial respiratory complex I (0.25 μmol/L, 25 μmol/L rotenone), and mitochondrial respiratory complex III (10 ng/mL, 1 μg/mL antimycin A). The expression of HIF-1α induced by hypoxia was unaffected by CHC and rapamycin (Fig. 4*A*), whereas it was completely blocked by rotenone and antimycin A (Fig. 4*B*). Moreover, rotenone and antimycin A increased the phosphorylation of AMPK-α and ACC and decreased the expression of *p*-mTOR (Fig. 4*B*).

Metformin decreased oxygen consumption and intracellular ATP levels. Having identified that metformin had similar effects on the expressions of hypoxia-induced HIF-1α protein and AMPK as mitochondrial respiratory inhibitors, we then directly measured the oxygen consumption and intracellular ATP levels in HRPTECs treated with 1 mmol/L metformin and 1 mmol/L AICAR under normoxic and hypoxic conditions in medium containing 5.5 mmol/L (low) or 25 mmol/L (high) glucose for 4 h. As shown in Fig. 4*C*, hypoxia decreased oxygen consumption down to 76.5% of the control in normoxia, which was consistent with the previous study (32), whereas this response to hypoxia was blunted by the treatment of 25 mmol/L glucose (Fig. 4*D*). Notably, metformin significantly inhibited oxygen consumption to <50% of controls, independent of the oxygen conditions or the glucose milieu (Fig. 4*C* and *D*). In addition, the results show that the trend was for cell ATP to decrease during metformin treatment under either normoxic or hypoxic conditions in contrast to the enhancement of ATP levels by the treatment of AICAR (Fig. 4*E*). Consistent with a previous study (33), hypoxia did not induce ATP depletion in HRPTECs because the metabolic shift to anaerobic glycolysis seems to have been sufficient to maintain ATP in hypoxic cells (Fig. 4*E*). In contrast, 25 mmol/L glucose attenuated ATP levels and the inhibitory effects of metformin on ATP levels in either normoxia or hypoxia (Fig. 4*F*).

Diphenylene, but not *N*-acetylcysteine, mimics the effects of metformin on AMPK-α and mTOR phosphorylation and on hypoxia-induced HIF-1α expression. Furthermore, we examined the effects of the NADPH oxidase inhibitor diphenylene iodonium (DPI) (10 μmol/L) and the antioxidant *N*-acetylcysteine (NAC) (5 mmol/L) on the expression of HIF-1α and the phosphorylation of AMPK-α and mTOR under normoxic and hypoxic conditions for 4 h. DPI, but not NAC, inhibited hypoxia-induced HIF-1α expression; increased the phosphorylation of AMPK-α and ACC; and decreased the phosphorylation of mTOR (Fig. 5*A*). Although DPI also has been known to inhibit the mitochondrial complex I (34,35), we measured NADPH content in order to evaluate whether the inhibition of NADPH oxidase by metformin was involved in the inhibitory effects of metformin on HIF-1α expression (Fig. 5*B*). Both metformin and AICAR recovered hypoxia-decreased NADPH content, suggesting that the inhibition of NADPH oxidase could not be attributed to the inhibitory effect of metformin.

Effects of metformin on reactive oxygen species production in HRPTECs. To investigate whether reactive oxygen species (ROS) production may be implicated in the inhibitory effects of metformin on HIF-1α expression, DHE staining was examined in HRPTECs. As shown in Fig. 5*C*, *upper panel*, hypoxia decreased DHE-associated fluorescence in the low-glucose medium compared with that under normoxic conditions. In the medium containing low glucose, metformin increased DHE staining independent of oxygen tension, as reported in the previous study (36), in contrast to AICAR (Fig. 5*C*). High glucose enhanced ROS production compared with low glucose, and metformin decreased high-glucose–induced ROS production, especially in normoxia (Fig. 5*C*, *lower panel*). Thus, these observations suggested that intracellular ROS production was not involved in the inhibitory effect of metformin on HIF-1α expression.

Metformin restored hypoxic conditions. Because metformin decreased oxygen consumption in HRPTECs, we investigated whether metformin increases intracellular oxygen tension using a hypoxia-sensitive dye, pimonidazole (Fig. 5*D*). Notably, metformin, but not AICAR, rescued the hypoxic state in HRPTECs under hypoxic conditions. In addition, immunocytochemical analysis confirmed that hypoxia apparently induced the nuclear expression of HIF-1α in HRPTECs compared with those in normoxia, and metformin inhibited hypoxia-induced HIF-1α nuclear stainings (Fig. 5*D*). AICAR did not evidently alter the expression of HIF-1α in HRPTECs under hypoxic conditions (Fig. 5*D*). We also examined the effects of metformin on the state of hypoxia in the kidney (Fig. 6*A* and *B*). The intensity of pimonidazole staining was increased in tubular cells of the kidney cortex of ZDF rats, which was significantly attenuated by metformin but not by insulin.

Metformin suppressed tubular HIF-1α expression in type 2 diabetic rats. To confirm the effects of metformin on tubular HIF-1α expression in vivo, we treated ZDF rats with metformin for 30 weeks. As expected, ZDF rats were hyperglycemic, and administration of metformin to ZDF rats significantly decreased HbA_{1c} by 24% ($P < 0.01$) (Table 1). ZDF rats had increased urinary volume and albumin excretion compared with lean controls, as described previously (23). Treatment of ZDF rats with metformin significantly prevented an increase in urinary albumin excretion to 58.3% of ZDF rats ($P < 0.05$) (Table 1). Consistent with the lack of albuminuria, ZL rats as lean controls showed neither glomerulosclerosis nor tubular injury (Fig. 6*C*, *d* and *e*). ZL rats exhibited the immunostainings of HIF-1α

results show that cell ATP in medium containing low glucose was trend to decrease during metformin treatment under either normoxic or hypoxic conditions in contrast to the enhancement of ATP production by the treatment of AICAR (*$P < 0.05$; **$P < 0.01$). *F*: In contrast, 25 mmol/L glucose attenuated ATP levels and the inhibitory effects of metformin on ATP levels in normoxia and hypoxia.

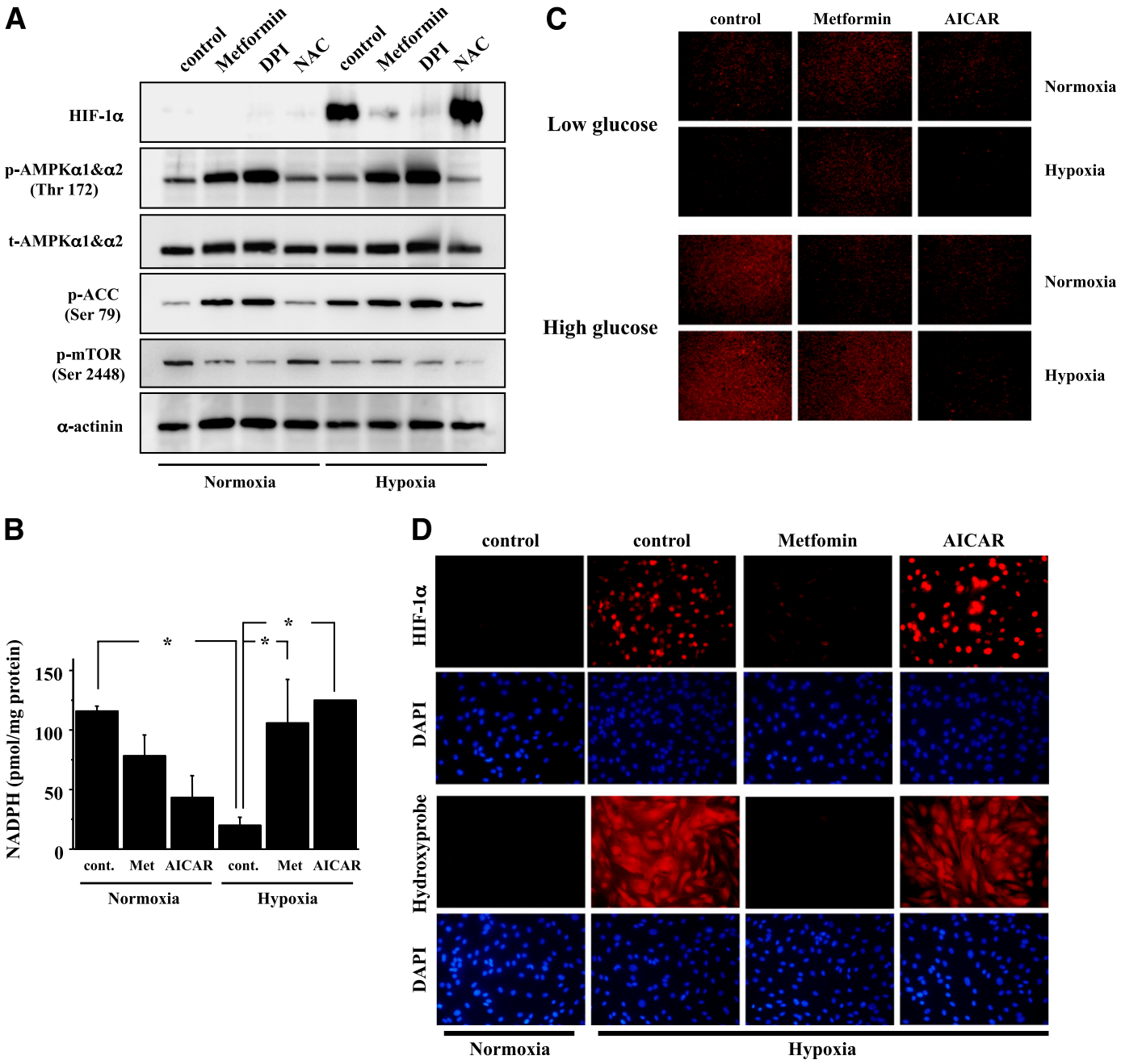

FIG. 5. ***A***: **An antioxidant, NAC, had no effect on hypoxia-induced HIF-1α protein expression. HRPTECs were treated with 1 mmol/L metformin, NADPH oxidase inhibitors (10 μmol/L DPI), the antioxidant (5 mmol/L NAC), and metformin under normoxic and hypoxic conditions for 4 h. NAC did not inhibit hypoxia-induced HIF-1α expression, indicating that mitochondrial ROS production was not involved in HIF-1α stabilization.** ***B***: **NADPH contents in HRPTECs. Both metformin and AICAR restored hypoxia-decreased NADPH contents. Data are expressed as means ± SD (n = 3). *P < 0.05.** ***C***: **Effects of metformin on ROS production in HRPTECs. Intracellular ROS were measured with DHE, which produces a red fluorescence in typically nuclear localization when oxidized to ethidium bromide by O_2^-. HRPTECs were treated with 1 mmol/L metformin or 1 mmol/L AICAR overnight under normoxic or hypoxic conditions in medium containing 5.5 mmol/L (low) or 25 mmol/L (high) glucose. In medium containing low glucose, hypoxia decreased DHE staining and metformin increased DHE staining in contrast to AICAR. High glucose enhanced DHE staining in normoxia and hypoxia. Metformin suppressed the high-glucose–induced ROS production in normoxia and did not increase DHE staining even under hypoxic conditions and in a high-glucose milieu (original magnification ×200).** ***D***: **Detection of the hypoxic state in HRPTECs. The cells were grown on the coverslides until subconfluence and then treated overnight as indicated. HRPTECs under normoxic conditions showed no staining for HIF-1α. Hypoxia induced nuclear expression of HIF-1α in HRPTECs, and 1 mmol/L metformin inhibited hypoxia-induced HIF-1α nuclear staining.** ***Upper panel***: **A total of 1 mmol/L AICAR did not affect the expression of HIF-1α in HRPTECs under hypoxic conditions.** ***Lower panel***: **Hypoxia of HRPTECs was detected by the use of pimonidazole hydrochloride. Metformin, not AICAR, increased cellular oxygen tension in HRPTECs under hypoxic conditions. Nuclei were stained with DAPI. Original magnification ×800. (A high-quality digital representation of this figure is available in the online issue.)**

only in the inner medullar tubules (Fig. 6*C*, *b*). Intriguingly, ZDF rats showed strong nuclear HIF-1α expression, especially in outer medullar and cortical proximal tubules in addition to the inner medulla (Fig. 6*C*, *f–h*), which is consistent with previous data in human diabetic kidney (8) and in the kidney of streptozotocin-induced diabetic rats (7). In addition, kidneys of ZDF rats showed glomerulosclerosis and tubulointerstitial injuries, as described previously (23)

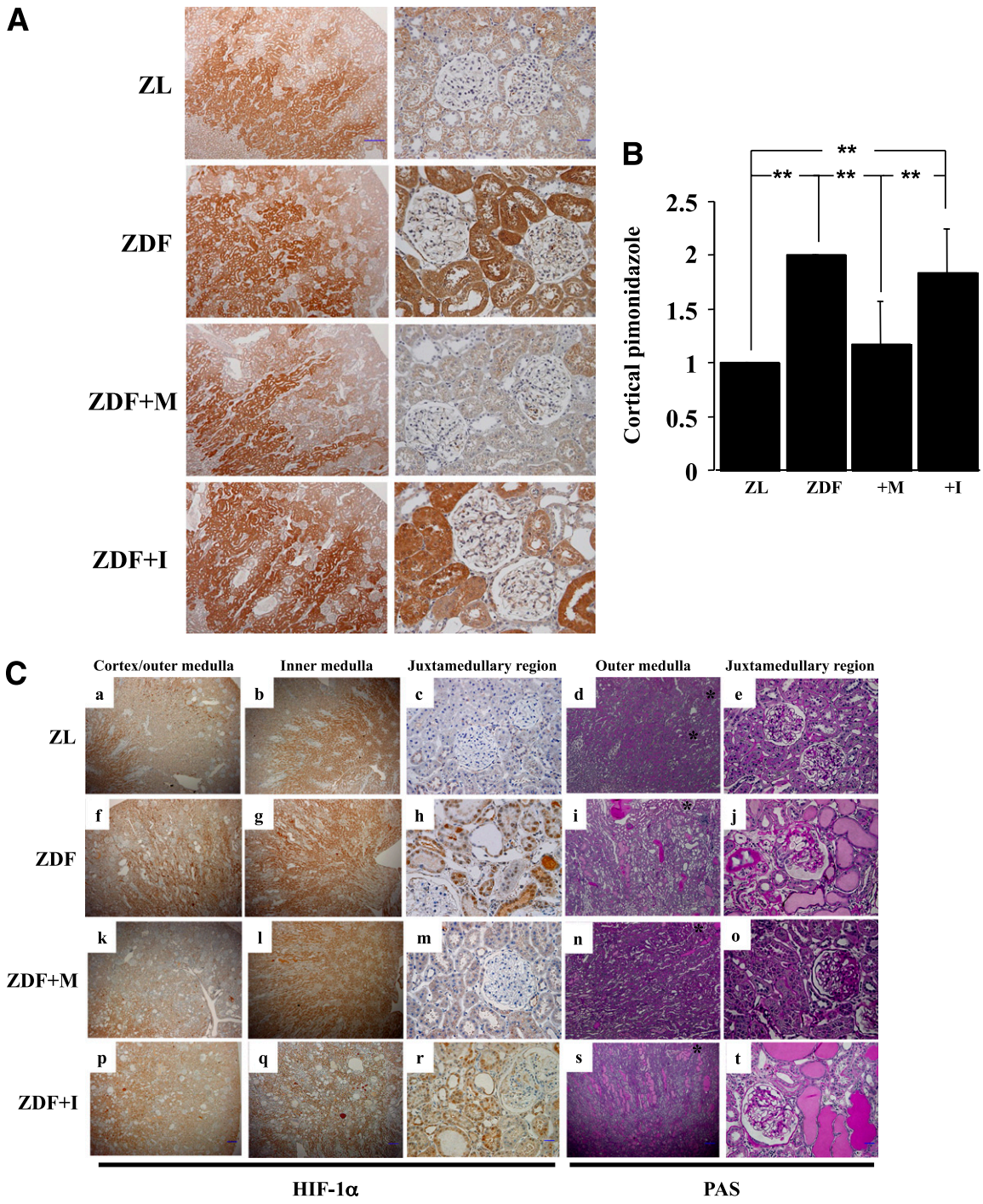

FIG. 6. ***A*****: Immunohistochemistry for the hypoxia marker pimonidazole. Rats were studied at 8 weeks of treatment by metformin or by insulin. Scar bars represent 300 μm (*left row*) and 30 μm (*right row*).** ***B*****: Intensity of pimonidazole staining was increased in tubular cells of the kidney cortex of ZDF, which was significantly attenuated by metformin treatment not by insulin. *****P*** **< 0.01.** ***C*****: Immunohistochemical analysis of HIF-1α expressions and light micrographs of sections from kidneys stained with the periodic acid–Schiff (PAS) reagent in Zucker lean control rats (ZL rats) (*a–e*), nontreated ZDF rats (ZDF) (*f–j*), metformin-treated ZDF rats (ZDF+M) (*k–o*), and insulin-treated ZDF rats (ZDF+I) (*p–t*). In the lean rats (*a–c*) and metformin-treated ZDF rats (*k–m*), HIF-1α–positive cells were renal tubular cells in the inner medulla, with few positive cells in the outer medulla and the cortex. In contrast, a marked increase in tubular staining for HIF-1α was observed in the outer medulla and cortex of ZDF rats (*f* and *h*). Lean control rats (ZL) showed no tubular and glomerular injury in kidneys (*d* and *e*). Notably, severe sclerosed glomeruli and damaged tubules, which present cellular debris, tubular cast formations, interstitial nephritis are observed in sections from ZDF rats (*i* and *j*). Metformin, but not insulin (*s* and *t*), ameliorated the tubular injury in the outer medulla and cortex of ZDF rats (*n* and *o*). Asterisks show the glomeruli. Scar bars represent 300 μm at low power field and 30 μm at high power field. (A high-quality digital representation of this figure is available in the online issue.)**

(Fig. 6*C*, *i* and *j*). Notably, positive immunostaining for HIF-1α was evidently decreased in kidneys of metformin-treated ZDF rats (Fig. 6*C*, *k* and *m*), accompanied by amelioration of the tubular injury (Fig. 6*C*, *n* and *o*), which was in contrast to those in kidneys of insulin-treated rats, as described in the previous study (37) (Fig. 6*C*, *p*, *r–t*). Semiquantitative assessment for HIF-1α immunostaining and injury in cortical and outer medullary tubules revealed

TABLE 1
Data collected at 39 weeks

	ZDF *fa/+* (lean)	ZDF *fa/fa* (diabetic)		
		Untreated	Metformin	Insulin
n	6	4	4	6
Body weight (g)	496.17 ± 13.48	403 ± 4.97	457 ± 61.52	631 ± 36.14*†‡
Food intake (g/day)	13.98 ± 3.11	39.81 ± 2.50*	33.63 ± 9.25*	22.38 ± 3.79*†‡
Fed glucose (mg/dL)	132.17 ± 15.33	573.50 ± 19.50*	451.00 ± 116.55*	296.33 ± 100.76*†‡
HbA_{1c} (%)	3.43 ± 0.27	10.38 ± 0.59*	7.88 ± 1.27*†	5.73 ± 1.15*†‡
Urine volume (mL/day)	8.55 ± 2.44	148.73 ± 11.61*	85.48 ± 48.77*†	32.92 ± 14.07†‡
Urinary albumin ($mg \cdot kg^{-1} \cdot day^{-1}$)	6.85 ± 3.48	349.44 ± 92.55*	203.80 ± 121.32*§	108.51 ± 45.69*†‖
HIF-α immunoreactivity	0.0 ± 0.0	2.0 ± 1.16*	0.5 ± 0.58§	1.17 ± 0.41¶
Tubular injury	0.0 ± 0.0	3.0 ± 0.0*	1.75 ± 0.96*†	2.5 ± 0.55*

Data are means ± SD unless otherwise indicated. *$P < 0.01$ vs. lean rats. †$P < 0.01$ vs. untreated diabetic rats. ‡$P < 0.01$ vs. metformin-treated rats. §$P < 0.05$; ‖$P < 0.05$; ¶$P < 0.05$.

that chronic metformin treatment significantly decreased HIF-1α expression and ameliorated tubular injury in ZDF rats (Table 1).

DISCUSSION

In this study, we found that metformin inhibits hypoxia-induced HIF-1α protein expression and thus the expression of its targeted genes, probably via the inhibition of mitochondrial respiration in HRPTECs.

Metformin has been found to activate AMPK, a major cellular regulator of lipid and glucose metabolism (16–18). Previous studies also have shown that metformin is an inhibitor of complex I of the mitochondrial respiratory chain (38,39), independent of the AMPK pathway (17,40).

To investigate the underlying mechanism(s) of the action of metformin, we first assessed the role of AMPK activation in hypoxia-induced HIF-1α expression, utilizing AICAR, compound C, and siRNA for AMPK-α1 or -α2. We found that metformin-induced AMPK phosphorylation was not related to HIF-1α inhibition. In addition, we show that metformin suppresses mitochondrial respiratory function, suggesting that the redistribution of intracellular oxygen is involved in the inhibitory effects of metformin on HIF-1α expression, as described in a previous study (41). Collectively, our results suggest that metformin inhibits HIF-1α expression through the suppression of mitochondrial respiration described as inhibition of oxygen consumption and intracellular ATP levels, which subsequently activates AMPK pathways, proposing that AMPK-α is a downstream regulator of the mitochondrial respiratory chain. That is probably the reason that an AMPK activator, AICAR, fails to inhibit hypoxia-induced HIF-1α expression.

AMPK activated by metformin has been reported to increase glucose transporter (GLUT-1 and GLUT-4) and glycolytic enzymes, thereby enhancing glycolytic glucose utilization (42), and to directly stimulate glycolysis in hypoxic or anoxic cells (43). Thus, metformin could promote Pasteur effects, which include decreased oxidative phosphorylation and an increase in anaerobic fermentation (44) by inhibiting mitochondrial respiration and increasing glucose uptake mediated by AMPK activation. Although metformin inhibits hypoxia-induced Glut-1 expression in HRPTECs, an HIF-1α–mediated increase in glucose uptake and metabolism during severe hypoxia is known not to be required for cell survival using cultured mouse primary renal proximal tubular cells (33). Intriguingly, high glucose increases oxygen consumption even under hypoxic conditions but fails to augment ATP production, indicating that high glucose abolishes Pasteur effects, which are adaptive responses to hypoxic stress, and that high glucose decreases mitochondrial efficiency by uncoupling oxygen consumption from ATP production. An HIF-1–dependent block to oxygen utilization results in increased oxygen availability and decreased cell death when total oxygen is limiting (32). Therefore, our findings suggest that in chronic hypoxia, as seen in diabetic nephropathy, metformin may rescue the renal proximal tubular cells from hypoxia, oxidative stress, and energy depletion by suppressing oxygen consumption via inhibition of mitochondrial respiratory chain complex I, instead of HIF-1, subsequently restoring Pasteur effects, which are impaired by hyperglycemia (Fig. 7).

In chronic kidney injury, including diabetic nephropathy, hypoxia promotes the development of renal fibrosis by inducing connective tissue growth factor (CTGF) (45) and

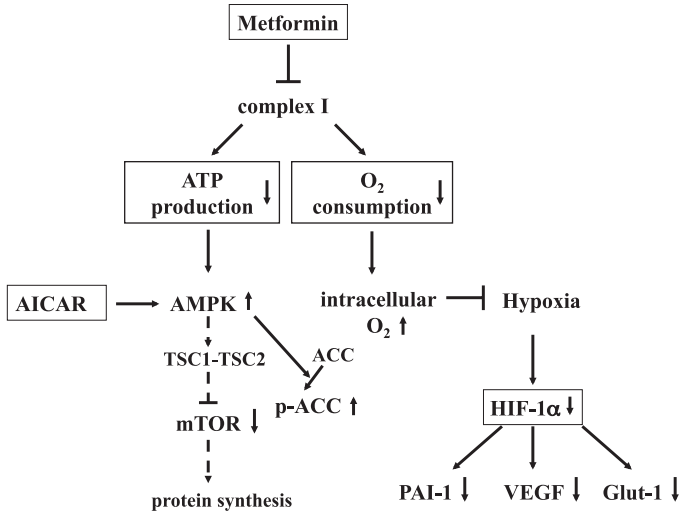

FIG. 7. Metformin inhibits hypoxia-induced HIF-1α protein expression through the inhibition of mitochondrial respiration. Metformin inhibits oxygen consumption and ATP production by inhibiting mitochondrial complex I. Subsequently, intracellular oxygen redistribution supplies oxygen for prolyl hydroxylase, which promotes the degradation of HIF-1α in the proteasome. ATP depletion caused by mitochondrial inhibition activates AMPK, which is a downstream signaling pathway of mitochondrial respiratory chain complex. Therefore, AICAR activates AMPK pathway but fails to inhibit hypoxia-induced HIF-1α accumulation.

EMT (8,9,46) through a HIF-1–dependent pathway in renal tubular cells by augmenting apoptosis of glomerular endothelial cells (47) and by upregulating matrix production and decreasing turnover in renal fibroblasts (48). Very recently, Kimura et al. (10) induced interstitial fibrosis in the kidney of aged $VHL^{-/-}$ mice, in which pronounced HIF-1α expression was observed in cortical tubular epithelial cells. They also demonstrated that the anti–HIF-1α agent [3-(5′-hydroxymethyl-2′-furyl)-1-benzyl indazole] (YC-1) ameliorated interstitial fibrosis in unilateral obstruction kidneys (10). We have shown that a preclinical study using ZDF rats confirmed the expression of HIF-1α in diabetic nephropathy, which has been described as the presence of hypoxia in previous studies (4–8), and explored the renoprotective effects of metformin in vivo.

In conclusion, these results in vitro and in vivo indicate, for the first time, that the antidiabetes drug metformin inhibits renal tubular HIF-1α expression. These data provide a novel mechanism of effects of metformin to improve microalbuminuria in diabetic nephropathy (14), protecting from hypoxia-induced renal fibrosis by attenuating the expression of HIF-1α (Fig. 7).

ACKNOWLEDGMENTS

No potential conflicts of interest relevant to this article were reported.

Y.T. researched data and wrote the manuscript. T.H. contributed to discussion. J.W., Y.F., and J.H. researched data. N.S. and Y.M. contributed to discussion. M.H. contributed to discussion and reviewed and edited the manuscript.

The authors are grateful to Ken Inoki (University of Michigan, Ann Arbor, MI) and Shin-ichi Araki (Shiga University of Medical Science) for helpful discussions. The authors also express their appreciation to Shinji Kume (Shiga University of Medical Science) for his technical assistance.

REFERENCES

1. Nangaku M. Chronic hypoxia and tubulointerstitial injury: a final common pathway to end-stage renal failure. J Am Soc Nephrol 2006;17:17–25
2. Haase VH. The VHL/HIF oxygen-sensing pathway and its relevance to kidney disease. Kidney Int 2006;69:1302–1307
3. Eckardt KU, Bernhardt W, Willam C, Wiesener M. Hypoxia-inducible transcription factors and their role in renal disease. Semin Nephrol 2007; 27:363–372
4. Singh DK, Winocour P, Farrington K. Mechanisms of disease: the hypoxic tubular hypothesis of diabetic nephropathy. Nat Clin Pract Nephrol 2008;4: 216–226
5. Ries M, Basseau F, Tyndal B, et al. Renal diffusion and BOLD MRI in experimental diabetic nephropathy. Blood oxygen level-dependent. J Magn Reson Imaging 2003;17:104–113
6. Palm F, Hansell P, Ronquist G, Waldenström A, Liss P, Carlsson PO. Polyol-pathway-dependent disturbances in renal medullary metabolism in experimental insulin-deficient diabetes mellitus in rats. Diabetologia 2004; 47:1223–1231
7. Rosenberger C, Khamaisi M, Abassi Z, et al. Adaptation to hypoxia in the diabetic rat kidney. Kidney Int 2008;73:34–42
8. Higgins DF, Kimura K, Bernhardt WM, et al. Hypoxia promotes fibrogenesis in vivo via HIF-1 stimulation of epithelial-to-mesenchymal transition. J Clin Invest 2007;117:3810–3820
9. Sun S, Ning X, Zhang Y, et al. Hypoxia-inducible factor-1α induces Twist expression in tubular epithelial cells subjected to hypoxia, leading to epithelial-to-mesenchymal transition. Kidney Int 2009;75:1278–1287
10. Kimura K, Iwano M, Higgins DF, et al. Stable expression of HIF-1α in tubular epithelial cells promotes interstitial fibrosis. Am J Physiol Renal Physiol 2008;295:F1023–F1029
11. Bailey CJ, Turner RC. Metformin. N Engl J Med 1996;334:574–579
12. UK Prospective Diabetes Study (UKPDS) Group. Effect of intensive blood-glucose control with metformin on complications in overweight patients with type 2 diabetes (UKPDS 34). Lancet 1998;352:854–865
13. Abbasi F, Chu JW, McLaughlin T, Lamendola C, Leary ET, Reaven GM. Effect of metformin treatment on multiple cardiovascular disease risk factors in patients with type 2 diabetes mellitus. Metabolism 2004;53: 159–164
14. Amador-Licona N, Guízar-Mendoza JM, Vargas E, Sánchez-Camargo G, Zamora-Mata L. The short-term effect of a switch from glibenclamide to metformin on blood pressure and microalbuminuria in patients with type 2 diabetes mellitus. Arch Med Res 2000;31:571–575
15. Pilmore HL. Review: metformin: potential benefits and use in chronic kidney disease. Nephrology (Carlton) 2010;15:412–418
16. Zhou G, Myers R, Li Y, et al. Role of AMP-activated protein kinase in mechanism of metformin action. J Clin Invest 2001;108:1167–1174
17. Hawley SA, Gadalla AE, Olsen GS, Hardie DG. The antidiabetic drug metformin activates the AMP-activated protein kinase cascade via an adenine nucleotide-independent mechanism. Diabetes 2002;51:2420–2425
18. Shaw RJ, Lamia KA, Vasquez D, et al. The kinase LKB1 mediates glucose homeostasis in liver and therapeutic effects of metformin. Science 2005; 310:1642–1646
19. Lee M, Hwang JT, Lee HJ, et al. AMP-activated protein kinase activity is critical for hypoxia-inducible factor-1 transcriptional activity and its target gene expression under hypoxic conditions in DU 145 cells. J Biol Chem 2002;278:39653–39661
20. Shackelford DB, Vasquez DS, Corbeil J, et al. mTOR and HIF-1alpha-mediated tumor metabolism in an LKB1 mouse model of Peutz-Jeghers syndrome. Proc Natl Acad Sci USA 2009;106:11137–11142
21. Lieberthal W, Levine JS. The role of the mammalian target of rapamycin (mTOR) in renal disease. J Am Soc Nephrol 2009;20:2493–2502
22. Treins C, Murdaca J, Van Obberghen E, Giorgetti-Peraldi S. AMPK activation inhibits the expression of HIF-1alpha induced by insulin and IGF-1. Biochem Biophys Res Commun 2006;342:1197–1202
23. Coimbra TM, Janssen U, Gröne HJ, et al. Early events leading to renal injury in obese Zucker (fatty) rats with type II diabetes. Kidney Int 2000;57: 167–182
24. Miyauchi K, Takiyama Y, Honjyo J, Tateno M, Haneda M. Upregulated IL-18 expression in type 2 diabetic subjects with nephropathy: TGF-beta1 enhanced IL-18 expression in human renal proximal tubular epithelial cells. Diabetes Res Clin Pract 2009;83:190–199
25. Bindokas VP, Jordán J, Lee CC, Miller RJ. Superoxide production in rat hippocampal neurons: selective imaging with hydroethidine. J Neurosci 1996;16:1324–1336
26. Smith AC, Mullen KL, Junkin KA, et al. Metformin and exercise reduce muscle FAT/CD36 and lipid accumulation and blunt the progression of high-fat diet-induced hyperglycemia. Am J Physiol Endocrinol Metab 2007; 293:E172–E181
27. Cleasby ME, Dzamko N, Hegarty BD, Cooney GJ, Kraegen EW, Ye JM. Metformin prevents the development of acute lipid-induced insulin resistance in the rat through altered hepatic signaling mechanisms. Diabetes 2004;53:3258–3266
28. Deji N, Kume S, Araki S, et al. Structural and functional changes in the kidneys of high-fat diet-induced obese mice. Am J Physiol Renal Physiol 2009;296:F118–F126
29. Frid A, Sterner GN, Löndahl M, et al. Novel assay of metformin levels in patients with type 2 diabetes and varying levels of renal function: clinical recommendations. Diabetes Care 2010;33:1291–1293
30. Hayashi T, Hirshman MF, Fujii N, Habinowski SA, Witters LA, Goodyear LJ. Metabolic stress and altered glucose transport: activation of AMP-activated protein kinase as a unifying coupling mechanism. Diabetes 2000; 49:527–531
31. Lee MJ, Feliers D, Mariappan MM, et al. A role for AMP-activated protein kinase in diabetes-induced renal hypertrophy. Am J Physiol Renal Physiol 2007;292:F617–F627
32. Papandreou I, Cairns RA, Fontana L, Lim AL, Denko NC. HIF-1 mediates adaptation to hypoxia by actively downregulating mitochondrial oxygen consumption. Cell Metab 2006;3:187–197
33. Biju MP, Akai Y, Shrimanker N, Haase VH. Protection of HIF-1-deficient primary renal tubular epithelial cells from hypoxia-induced cell death is glucose dependent. Am J Physiol Renal Physiol 2005;289:F1217–F1226
34. Hutchinson DS, Csikasz RI, Yamamoto DL, et al. Diphenylene iodonium stimulates glucose uptake in skeletal muscle cells through mitochondrial complex I inhibition and activation of AMP-activated protein kinase. Cell Signal 2007;19:1610–1620
35. Lambert AJ, Buckingham JA, Boysen HM, Brand MD. Diphenyleneiodonium acutely inhibits reactive oxygen species production by mitochondrial complex I during reverse, but not forward electron transport. Biochim Biophys Acta 2008;1777:397–403

36. Anedda A, Rial E, González-Barroso MM. Metformin induces oxidative stress in white adipocytes and raises uncoupling protein 2 levels. J Endocrinol 2008;199:33–40
37. Ohtomo S, Izuhara Y, Takizawa S, et al. Thiazolidinediones provide better renoprotection than insulin in an obese, hypertensive type II diabetic rat model. Kidney Int 2007;72:1512–1519
38. El-Mir MY, Nogueira V, Fontaine E, Avéret N, Rigoulet M, Leverve X. Dimethylbiguanide inhibits cell respiration via an indirect effect targeted on the respiratory chain complex I. J Biol Chem 2000;275:223–228
39. Owen MR, Doran E, Halestrap AP. Evidence that metformin exerts its anti-diabetic effects through inhibition of complex 1 of the mitochondrial respiratory chain. Biochem J 2000;348:607–614
40. Foretz M, Hébrard S, Leclerc J, et al. Metformin inhibits hepatic gluconeogenesis in mice independently of the LKB1/AMPK pathway via a decrease in hepatic energy state. J Clin Invest 2010;120:2355–2369
41. Hagen T, Taylor CT, Lam F, Moncada S. Redistribution of intracellular oxygen in hypoxia by nitric oxide: effect on HIF1α. Science 2003;302:1975–1978
42. Fujii N, Jessen N, Goodyear LJ. AMP-activated protein kinase and the regulation of glucose transport. Am J Physiol Endocrinol Metab 2006;291:E867–E877
43. Hue L, Beauloye C, Bertrand L, et al. New targets of AMP-activated protein kinase. Biochem Soc Trans 2003;31:213–215
44. Hochachka PW, Buck LT, Doll CJ, Land SC. Unifying theory of hypoxia tolerance: molecular/metabolic defense and rescue mechanisms for surviving oxygen lack. Proc Natl Acad Sci USA 1996;93:9493–9498
45. Higgins DF, Biju MP, Akai Y, Wutz A, Johnson RS, Haase VH. Hypoxic induction of Ctgf is directly mediated by Hif-1. Am J Physiol Renal Physiol 2004;287:F1223–F1232
46. Manotham K, Tanaka T, Matsumoto M, et al. Transdifferentiation of cultured tubular cells induced by hypoxia. Kidney Int 2004;65:871–880
47. Tanaka T, Miyata T, Inagi R, et al. Hypoxia-induced apoptosis in cultured glomerular endothelial cells: involvement of mitochondrial pathways. Kidney Int 2003;64:2020–2032
48. Norman JT, Clark IM, Garcia PL. Hypoxia promotes fibrogenesis in human renal fibroblasts. Kidney Int 2000;58:2351–2366